Photoelectron angular distribution and linear magnetic dichroism in the $4p$ photoemission from Rb atoms

J. Niskanen,[1,2] S. Urpelainen,[1] K. Jänkälä,[1] J. Schulz,[1,3] S. Heinäsmäki,[1] S. Fritzsche,[1,4] N. M. Kabachnik,[1,5] S. Aksela,[1] and H. Aksela[1]

[1]*Department of Physics, University of Oulu, SPO Box 3000, FIN-90014, Finland*

[2]*Department of Theoretical Chemistry, School of Biotechnology, Royal Institute of Technology, Stockholm, Sweden*

[3]*Center for Free-Electron-Laser Science (CFEL) at DESY, D-22603 Hamburg, Germany*

[4]*GSI Helmholzzentrum für Schwerionenforschung, D-64291 Darmstadt, Germany*

[5]*Institute of Nuclear Physiscs, Moscow State University, Moscow RU-119991, Russia*

(Received 11 November 2009; published 12 January 2010)

The angular distribution of photoelectrons and linear magnetic dichroism in the angular distribution for the $4p$ photoemission from Rb atoms in the ground state, oriented by laser pumping, were measured in the photon energy range from 50 to 100 eV. The experimental results are compared with the multiconfiguration Dirac-Fock (MCDF) calculations. We show that the zero-crossing of the dichroism as a function of energy is connected with the Cooper minimum in the cross section. This fact can be used for an accurate determination of the position of the Cooper minimum.

DOI: 10.1103/PhysRevA.81.013406 PACS number(s): 32.80.Fb, 32.80.Xx

I. INTRODUCTION

Angle-resolved photoelectron spectroscopy in combination with laser optical pumping has proved to be a powerful method for studying the photoionization dynamics of atoms [1]. In recent years this method was successfully applied to various targets and among them to alkali-metal atoms [2–12]. In alkali-metal atoms, the first excited state, corresponding to the transition $ns \rightarrow np$, lies within the energy range that is easily achievable by optical lasers. Because of this, the experiments with laser-excited and polarized alkali-metal atoms, and especially with Na atoms, have become a showcase for such types of investigations. Completely fine-structure-resolved photoelectron spectra from laser-excited Na atoms were reported by Cubaynes *et al.* [2]. Shakedown satellites in the $2p$-photoelectron emission of laser-excited Na atoms were investigated by Schulz *et al.* [3]. Recently, linear alignment dichroism and linear magnetic dichroism were studied for the $2p$ photoionization of laser-pumped ground and excited states of Na atoms [4,5]. Jänkälä *et al.* [6] investigated the $2p$ photoionization and subsequent Auger decay spectra from laser-excited K. High-resolution photoelectron spectra of laser-excited K atoms in the region of $3p^5 4p$ states were measured and theoretically analyzed by Meyer *et al.* [7]. Also, heavier alkali-metal atoms Rb and Cs were studied by this method [8–12]. In particular, the fine-structure-resolved $4p$ photoemission of free Rb atoms in the ground state and following their excitation into the $[\mathrm{Kr}]5p\ ^2P_{1/2}$ and $^2P_{3/2}$ states were investigated in Ref. [10].

Laser pumping of atomic states is usually accompanied by their polarization. Pumping by linearly polarized laser light can lead to alignment of the excited and/or the ground state if the total angular momentum of the states is $J \geqslant 1$. A circularly polarized laser can produce orientation of the target atom if $J \geqslant 1/2$. Subsequent photoionization of the polarized atoms by synchrotron radiation (SR) exhibit dichroism of different types [13,14]. In particular, if the laser beam is circularly polarized, the change from right-hand to left-hand circular polarization leads to the inversion of the target-atom orientation, which in turn results in the difference of photoelectron angular distributions, usually called magnetic dichroism in the angular distribution. If the ionizing synchrotron beam is linearly polarized then the previously described dichroism is called linear magnetic dichroism in the angular distribution (LMDAD). Similarly, if the target atom is aligned by linearly polarized laser light in two perpendicular directions, the difference in the photoelectron angular distribution is called linear alignment dichroism in the angular distribution (LADAD). In recent years, the already mentioned types of dichroism have been extensively studied both experimentally and theoretically (see Ref. [1] and references therein) and provided rich information about electron correlations in atoms and photoionization dynamics.

The present article is devoted to the experimental and theoretical study of photoelectron angular distribution and linear magnetic dichroism in $4p$ photoionization of free Rb atoms in the ground state, oriented by laser-pumping. To the best of our knowledge this is the first measurement of this type for Rb. We also investigate for the first time the dependence of the LMDAD on the exciting-photon energy. The article is organized as follows. The next section describes the experimental set-up. The theoretical background is given in Sec. III, where we present and discuss all formulas necessary for the analysis of the experimental data. We also describe the model used for the description of photoionization of Rb atoms. In Sec. IV we present and discuss the experimental results and compare them with our calculations. Conclusions are given in Sec. V.

II. EXPERIMENTAL SETUP

The experiments were carried out on the high-resolution soft-x-ray undulator beamline I411 on the 1.5 GeV MAX II electron storage ring in MAX-laboratory (Lund, Sweden) [15]. For the purposes of studying the angular anisotropy, the Rb photoelectron spectra were recorded using the permanent Scienta R4000 end-station mounted at the end of the beamline.

To record the photoelectron spectra from the laser-pumped atoms a modified Scienta SES-100 electron analyzer with a resistive-anode position-sensitive detector [16,17] mounted on the so-called 1 m section of the beamline was used.

To produce the atomic Rb vapor a resistively heated thermocoax oven with a stainless steel crucible built in Oulu was used in both experiments. The temperature of the oven was monitored using a thermocouple placed slightly below the crucible and the temperature was kept constant at around 110°C. This corresponds to a vapor pressure roughly in the order of 10^{-4}–10^{-3} mbar within the heated volume [18]. The Rb sample with a purity of 99.9+% was purchased from STREM Chemicals, Inc. and was stored in prescored glass ampoules.

The photoelectron spectra for determining the angular anisotropy parameters were recorded at a constant pass energy of 50 eV and analyzer entrance slit of 0.5 mm (curved) corresponding to an analyzer contribution of approximately 65 meV in the observed linewidth. The spectra were recorded at photon energies of 50, 60, 72, and 100 eV. The exit slit of the monochromator was chosen to be 100 μm, corresponding to a photon bandwidth of roughly 30, 40, 55, and 85 meV for the various photon energies, respectively. To determine the angular anisotropy parameter β the spectra were recorded at three different angles with respect to the electric-field vector of the incoming horizontally linearly polarized radiation. The chosen emission angles were 0°, 30°, and 54.7°.

To account for possible instabilities in the photon-beam and electron-analyzer transmission effects at different kinetic energies, as well as at different emission angles due to the off-center rotation of the electron energy analyzer about the photon beams, the He 2*s* photoline was recorded for normalization purposes together with the Rb photolines. The He line also serves as an important calibration source as their β value is a well-known constant 2 at all photon energies. As the He lines overlap slightly with satellite lines from the Rb photoionization, the spectra were recorded both with and without He and the pure He signal was subtracted for normalization. The He gas was introduced to the chamber via free expansion through a pipe at the base of the oven and the gas pressure was kept constant around 5×10^{-7} mbar throughout the measurements with variations less than 0.3×10^{-7} mbar. The background pressure was in the order of 4×10^{-8} mbar. For normalization, it was assumed that the relative amount of Rb and He in the interaction region remained constant throughout the experiments due to stable gas pressure and oven temperature.

The photoelectron spectra from laser-pumped atoms were recorded using a constant electron analyzer pass energy of 10 eV with an entrance slit of 0.8 mm (curved). This corresponds to an analyzer broadening of approximately 40 meV. The monochromator exit slit was 50 μm and the corresponding bandwidth 20, 25, 26, 28, 30, and 45 meV for photon energies 60, 70, 72, 75, 80, and 100 eV, respectively. The spectra were recorded at an electron emission angle of 45° with respect to the polarization vector of the incoming SR beam in the plane perpendicular to the beams.

The laser radiation was produced using a commercial Coherent 899 Ti:Sa laser pumped by a 10 W Coherent Verdi Nd Vanadate laser operating at 532 nm in multimode [8]. The output power at the desired excitation wavelength 780 nm corresponding to Rb $5s \rightarrow 5p_{3/2}$ resonance was measured to be around 1.2 W directly after the laser; the laser was focused to a spot of approximately 2 mm in diameter. Both left-handed and right-handed circular polarization of the laser radiation were used and the polarization state was changed from the natural linear polarization produced by the laser to a circular polarization using a quarter wave plate after the laser optics. The SR beam and laser beam were made colinear using the visible zero-order light from the synchrotron and overlapping the two beams, both at the entrance to the vacuum chamber, directly after the laser, and in between the two. The stability of the laser was monitored by recording the intensity of the fluorescence signal from the sample using a photodiode mounted on the experimental chamber. The detuning of the laser was not significant during the recording of any given set of data.

III. THEORETICAL BACKGROUND

Angular distribution of photoelectrons emitted from a polarized target atom with the angular momentum J_0 (other quantum numbers characterizing the initial atomic state are denoted α_0) can be presented in the following form [19,20]

$$\frac{d\sigma}{d\Omega} = \pi\alpha\omega(3\hat{J}_0)^{-1} \sum_{k_0 k k_\gamma} \rho_{k_0 0}(\alpha_0 J_0) B_{k_0 k k_\gamma} \times F_{k_0 k k_\gamma}(\vartheta_a, \varphi_a, \vartheta_e, \varphi_e;\ P_1, P_2, P_3). \quad (1)$$

Here α is the fine-structure constant, ω is the frequency of the ionizing photon, $B_{k_0 k k_\gamma}$ are the dynamical coefficients that contain the photoionization amplitudes, $\rho_{k_0 0}(\alpha_0 J_0)$ are the statistical tensors characterizing the polarization of the initial atomic state, and $F_{k_0 k k_\gamma}(\vartheta_a, \varphi_a, \vartheta_e, \varphi_e;\ P_1, P_2, P_3)$ are the kinematical factors, given by Eq. (14) of Ref. [19], which contain the Stokes parameters of the SR (P_1, P_2, P_3), emission angles of the photoelectrons ϑ_e, φ_e, and the direction of the target polarization axis ϑ_a, φ_a (axial symmetry is implied for the polarized target atom). The dynamical coefficients $B_{k_0 k k_\gamma}$ may be expressed as follows:

$$B_{k_0 k k_\gamma} = 3\ \hat{J}_0 \sum_{\substack{J J' \\ l l' j j'}} (-1)^{J+J_f+k_\gamma-1/2} \hat{J}\hat{J}'\hat{j}\hat{j}'\hat{l}\hat{l}'\ (l0, l'0\,|\,k0) \times \begin{Bmatrix} j & l & \frac{1}{2} \\ l' & j' & k \end{Bmatrix} \begin{Bmatrix} j & J & J_f \\ J' & j' & k \end{Bmatrix} \begin{Bmatrix} J_0 & 1 & J \\ J_0 & 1 & J' \\ k_0 & k_\gamma & k \end{Bmatrix} M_{lj J} M^*_{l' j' J'}, \quad (2)$$

where we use the standard notations for the Wigner $6j$ and $9j$ coefficients, $\hat{j} \equiv \sqrt{2j+1}$, and $M_{lj J} \equiv \langle \alpha_f J_f, lj : J \,||\, \mathcal{D} \,||\, \alpha_0 J_0 \rangle$ is the reduced dipole matrix element that describes the transition from the initial state $\alpha_0 J_0$ to the final ionic state $\alpha_f J_f$ with the emission of a photoelectron with the orbital and total angular momenta l, j.

The summation in Eq. (1) is over all possible values of k_0, k, and k_γ, connected by a "triangle inequality"

$$|k_0 - k_\gamma| \leqslant k \leqslant k_0 + k_\gamma. \quad (3)$$

In addition, they are limited by the conditions

$$k_0 \leqslant 2J_0, \quad k_\gamma \leqslant 2, \quad k = \text{even}, \tag{4}$$

the latter being a consequence of the parity conservation in photoionization. Therefore, the number of terms in the sum (1) is limited.

If the target atom is unpolarized, the anisotropy of the photoelectron emission is determined by only one dynamical parameter, B_{022}. In this case, the angular distribution of photoelectrons produced by linearly polarized radiation can be presented in a standard form (the z axis is chosen along the photon polarization)

$$\frac{d\sigma}{d\Omega} = \frac{\sigma}{4\pi}\left[1 + \beta P_2(\cos\vartheta_e)\right]. \tag{5}$$

Here σ is the angle-integrated photoionization cross section and β is the anisotropy coefficient

$$\beta = -\sqrt{\frac{10}{3}} B_{022}/B_{000}. \tag{6}$$

LMDAD is defined as the difference of the cross sections (1) for the two opposite directions of the target orientation. In the described experiment, the orientation of the target ground state is produced by laser optical pumping with right (+) and left (−) circularly polarized light, which, in our convention, correspond to helicity +1 and −1, respectively. Thus we define the relative LMDAD as

$$\text{LMDAD} = \left[\left(\frac{d\sigma}{d\Omega}\right)^{+} - \left(\frac{d\sigma}{d\Omega}\right)^{-}\right] \Bigg/ \left[\left(\frac{d\sigma}{d\Omega}\right)^{+} + \left(\frac{d\sigma}{d\Omega}\right)^{-}\right]. \tag{7}$$

In the considered case of the laser-pumped ground state of a Rb atom with $J_0 = 1/2$, the target atoms can be only oriented and their orientation is described by the only nonzero tensor of the first rank ρ_{10}. Using the previously described formalism of Baier *et al.* [19] and taking into account the geometry of the experiment (counterpropagating laser and SR beams, the detector in the plane perpendicular to the beams at an angle 45° relative to the SR polarization) one obtains the following expression for the relative LMDAD

$$\text{LMDAD} = i\frac{\sqrt{15}}{2}\,\frac{\mathcal{A}_{10}\beta_{122}}{1+\beta/4}, \tag{8}$$

where $\mathcal{A}_{10} = \rho_{10}(\alpha_0 J_0)/\rho_{00}(\alpha_0 J_0)$ is the orientation parameter of the initial atomic $^2S_{1/2}$ state of Rb and $\beta_{122} = \sqrt{3}B_{122}/B_{000}$ is the dynamical coefficient. Obviously, β_{122} is imaginary since LMDAD is real. Note that LMDAD is purely an interference effect. As follows from Eq. (2), the squares of matrix elements do not contribute to the B_{122} coefficient (one can easily prove it using the properties of $9j$ symbols). Therefore, if only one channel contributes to the photoionization process (only one amplitude is nonzero) then LMDAD vanishes.

To calculate the β parameter and the LMDAD, the dipole amplitudes M_{ljJ} need to be evaluated for the photo transitions from the given initial bound state $|\psi_0\rangle = |\psi(\alpha_0\pi_0 J_0)\rangle$ with total angular momentum J_0 and parity π_0 to one of the final scattering states $|\psi_t\rangle$ with angular momentum J and parity π, respectively. These scattering states belong to different one-electron continua of the next highest charge state and are obtained by coupling the $4p$ hole state $|\psi_f\rangle = |\psi(\alpha_f\pi_f J_f)\rangle$ of the photoion with some partial wave of the outgoing electron with energy ϵ and the (one-electron) angular momentum

$$\kappa = \pm(j + 1/2) \qquad \text{with} \qquad l = j \pm 1/2.$$

In calculating these dipole amplitudes, of course, the main emphasis has to be placed on the construction of the initial and final-ionic (bound) states to include the electronic correlations to a sufficiently large extent.

For the inner-shell photoionization of open-shell atoms, the multiconfiguration Dirac-Fock (MCDF) method [21,22] has been found to be a versatile tool to calculate wave functions and transition amplitudes of various kinds [23,24]. In this method, an atomic state is approximated by a linear combination of so-called configuration state functions (CSF) of the same symmetry

$$|\psi_\alpha(\pi J)\rangle = \sum_{r=1}^{n_c} c_r(\alpha)|\,\gamma_r \pi J\rangle, \tag{9}$$

where n_c is the number of CSF and $\{c_r(\alpha)\}$ the representation of the state in the given many-electron basis. In ansatz (9), moreover, γ_r represents the occupation of the atomic shells as well as all further quantum numbers from the coupling of these shells that are required for a unique specification of the (bound) N-electron basis. In most standard computations, the CSF are constructed as antisymmetrized products of a common set of orthonormal orbitals and are optimized using the Dirac-Coulomb Hamiltonian. Further relativistic contributions to the representation $\{c_r(\alpha)\}$ of the atomic states can be added for medium and heavy elements and often help to improve their low-lying level structure and transition amplitudes. For Rb, we incorporated the low-frequency Breit interaction into the Hamiltonian matrix but left out further relativistic corrections [25]. The continuum spinors are then solved within a spherical and level-dependent potential of the final ion, a scheme that includes the exchange interaction of the emitted electron with the bound-state density [26]. The bound-state orbitals were generated by the MCDF method [21]. The diagonalization of the Dirac-Coulomb Hamiltonian was performed by means of the RATIP [27] program and the calculation of transition amplitudes M_{ljJ} was performed by its recently developed PHOTO component [28]. The differential cross sections for LMDAD and the angular distribution parameters were calculated utilizing the code by Heinäsmäki *et al.* [29].

Beside the $3d^{10}5s^2S_{1/2}$ ground state of Rb, the $26\,4p^5(5s + 4d)\ J = 0, 1, 2$ final states of the photoion were generated independently in two different computational models based on ansatz (9): (A) by using only the single nonrelativistic configuration $4p^5 5s$, and (B) by including, in addition, the $4p^5(5s + 4d)$ configuration. In both models, however, the same $1s \cdots 4s$ core shells were used and only the $4d$ orbitals were optimized in addition. While model A gives just rise to the four main peaks in the photoelectron spectrum in the limited-energy range considered, model B accounts for all five observed peaks (seven levels) in the spectrum (see Sec. IV). Although such a rather limited expansion does not enable one to "monitor" the convergence of the

angular and dichroism parameters, it enabled us to identify and analyze the observations as a function of the photon energy.

IV. RESULTS AND DISCUSSION

In Fig. 1, the part of the measured Rb $4p$-photoionization spectrum relevant to the following discussion is shown. The measurement was performed for the photon energy 60 eV at the "magic"emission angle ($\vartheta_e = 54.7^\circ$) with respect to the SR polarization vector. The spectrum practically coincides with that presented in Ref. [8]. Lines 1 and 2 are assigned using the jK-coupling scheme as $4p^5(^2P_{3/2})5s[3/2]_{J_f}$ with $J_f = 2$ and $J_f = 1$, respectively [30]. The next two lines, 3 and 4, correspond to the final ionic states $4p^5(^2P_{1/2})5s[1/2]_{J_f}$ with $J_f = 0$ and $J_f = 1$, respectively. Finally, line 5 is attributed to the configuration $4p^5 4d$ [8]. Note that we use these assignments as labels only. The theoretical results presented in the following are obtained within the MCDF approach, thus each ionic state is a mixture of relativistic configurations, which cannot be described in terms of a pure coupling scheme. The calculated spectrum in this energy range is represented by bars in Fig. 1. Note that all theoretical energies have been shifted by 0.86 eV to match the experiment. Although the spread of the calculated spectral lines is slightly larger than in the experiment, the structure of the spectrum is reproduced rather well, with line 5 being a composition of several strong correlation satellite lines with the dominant configuration $4p^5 4d$.

A. Angular distribution of photoelectrons

In Fig. 2 the anisotropy parameter β of the angular distribution of photoelectrons from Rb atoms is presented as a function of the photon energy for the two final states of Rb^+ ion $4p^5(^2P_{3/2})5s[3/2]_{2,1}$ (lines 1 and 2). The experimental error bars include statistical errors and errors due to the off-center rotation of the electron energy analyzer about the photon

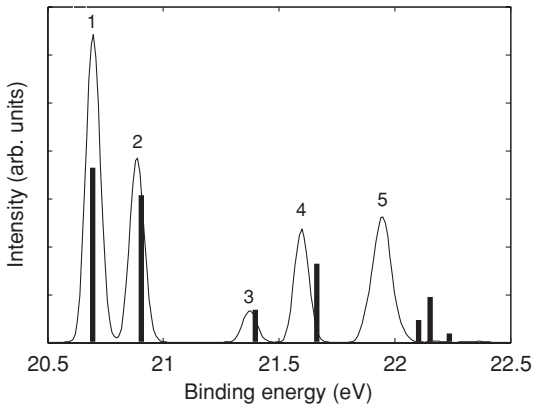

FIG. 1. The part of the experimental $4p$-photoemission spectrum of Rb studied (solid curve). Lines 1 and 2 are assigned as $4p_{3/2}^{-1}5s$ with $J_f = 2$ and 1, respectively, lines 3 and 4 belong to the ionic multiplet $4p_{1/2}^{-1}5s$ $J_f = 0$ and 1, respectively. Line 5 is attributed to the configuration $4p^{-1}4d$. The bars represent the theoretical spectrum calculated within the MCDF approach. For more details see the text.

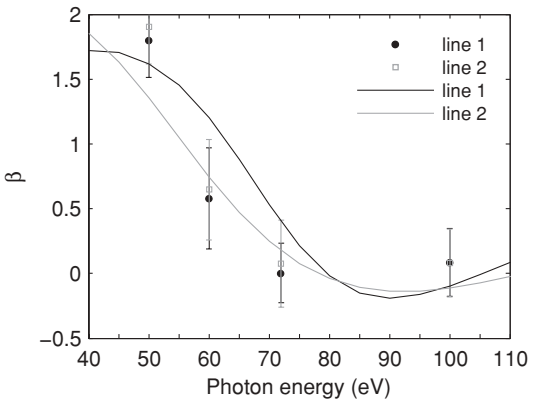

FIG. 2. Angular anisotropy parameter β as a function of photon energy for the $4p$ photoionization of the ground state of the Rb atom with transition to the $4p^5(^2P_{3/2})5s[3/2]_2$ (line 1) and $4p^5(^2P_{3/2})5s[3/2]_1$ (line 2) states of Rb^+ ion. The curves show the calculated results. The experimental data are shown by symbols with error bars.

beams. The measured angular distributions are quite similar for both spectral lines. The calculated β parameters for the two lines differ slightly more from each other than in the experiment, especially at the photon energies 50–75 eV. In general, the energy dependence of β parameters is reproduced rather well by the calculations, although for the first line the calculated curve is shifted toward higher energies by about 10 eV. The minimum of the β parameter is related to the Cooper minimum [31] in the photoionization cross section. In the Cooper minimum, the matrix element for one of the two contributing nonrelativistic partial waves (d wave) turns to zero. The remaining s wave gives an isotropic angular distribution (i.e., $\beta = 0$). The energy position of the Cooper minimum seems to be predicted by our theory at slightly larger energy than in the experiment. Note that, in our calculations, we disregard the effect of channel coupling in the continuum. As was demonstrated by Tulkki *et al.* [32] for the $4p$ photoionization of Kr, which is very close to the present case, the channel coupling can shift the position of the Cooper minimum by several eV. This may improve the agreement between theory and experiment.

B. Linear magnetic dichroism in the angular distribution

In Fig. 3(a) two photoelectron spectra for the $4p$ photoionization of the ground state of free Rb atoms measured at an angle 45° to the SR linear polarization are presented. The spectra differ by the helicity of the circularly polarized laser light used for pumping the transition $^2S_{1/2} \rightarrow {}^2P_{3/2}$ (780 nm). The pumping by circularly polarized light leads to orientation of the ground state, which reverses when the laser light is switched from right-hand to left-hand circular polarization. The shown spectra, measured at the photon energy of 60 eV, clearly exhibit effects of LMDAD. The strongest LMDAD effect is observed for the first two lines in the spectrum with binding energies of 20.71 and 20.90 eV [30]. The dichroism for line 2 has an opposite sign to that for line 1. For the second doublet, the dichroism is smaller and the signs of the dichroism are reversed. This fact can be easily explained using

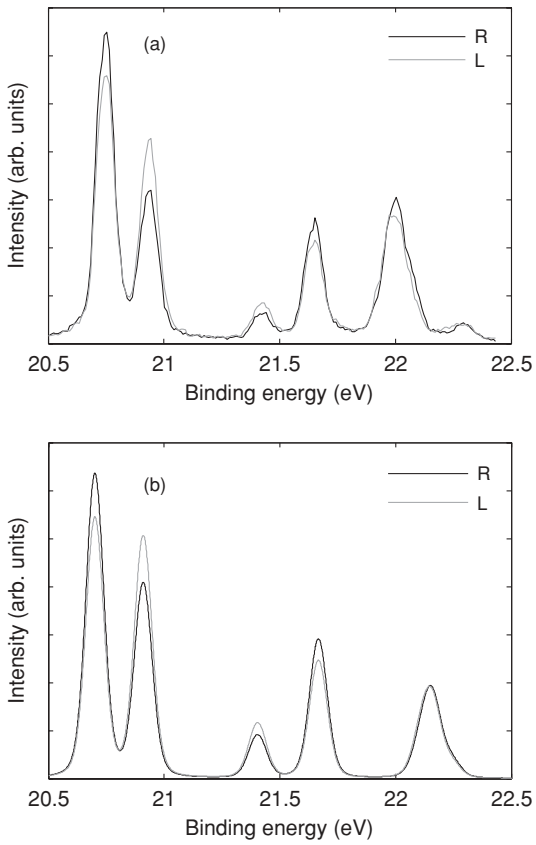

FIG. 3. (a) The experimental $4p$-photoelectron spectrum from the Rb ground state pumped by right (black curve) and left (gray curve) circularly polarized laser light, measured at the photon energy of 60 eV. (b) The corresponding theoretical spectra.

the geometrical model for the spectral patterns of dichroism, developed in Refs. [33,34]. As was shown, for the case of a pure coupling scheme, the dynamical coefficients $B_{k_0kk_\gamma}$ may be presented as a product of two factors and only one of them depends on quantum numbers of the entire atom. In particular, for the jK-coupling scheme, which is appropriate for the Rb ion, $B_{k_0kk_\gamma}$ are proportional to the factor $C_{k_0}(j_0, K_f, J_f)$ given by Eq. (15) of Ref. [34]. In the case of LMDAD for the considered transitions from the ground state $^2S_{1/2}$, this expression can be simplified to the following:

$$C_1(j_0, K_f, J_f) = 3\sqrt{2}\hat{J}_f^2\hat{j}_0^2(-1)^{J_f+l_0+1} \times \begin{Bmatrix} j_0 & j_0 & 1 \\ l_0 & l_0 & \frac{1}{2} \end{Bmatrix} \begin{Bmatrix} j_0 & j_0 & 1 \\ \frac{1}{2} & \frac{1}{2} & J_f \end{Bmatrix}, \quad (10)$$

where l_0 and j_0 are the orbital and the total angular momenta of the produced vacancy and $\hat{J} \equiv \sqrt{2J+1}$. In our particular case of $4p$ photoionization ($l_0 = 1$), one gets for $j_0 = 3/2$ (lines 1 and 2) $C_1 = \frac{5\sqrt{2}}{2}$ and $-\frac{5\sqrt{2}}{2}$ for $J_f = 2$ and 1, respectively. For $j_0 = 1/2$ (lines 3 and 4) similarly $C_1 = -2\sqrt{2}$ and $2\sqrt{2}$ for $J_f = 0$ and 1, respectively. This explains qualitatively the observed variation of the LMDAD effect for the considered lines.

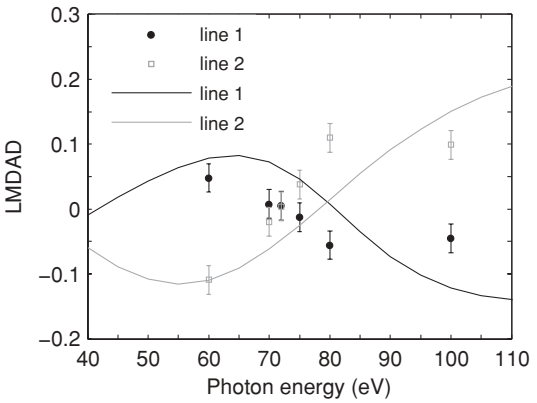

FIG. 4. Relative LMDAD as a function of photon energy for the two final ionic states $4p^5(^2P_{3/2})5s[3/2]_{2,1}$ (lines 1 and 2). Curves represent the results of calculations, points with error bars show the experimental data.

The results of the corresponding MCDF calculations are presented in Fig. 3(b). The theoretical dichroism depends on the value of orientation parameter $\mathcal{A}_{10}$ (see Eq. (8)) which was chosen to be 0.25 to give a good agreement with the experiment. This value implies that the ratio of the populations of the magnetic substates with projections $M = +\frac{1}{2}$ and $M = -\frac{1}{2}$ is 62.5:37.5. The spectra, presented in Fig. 3(b), were obtained from the theoretical intensities by convolution with Gaussian and Lorentzian line shapes with full width at half maximum (FWHM) 80 and 10 meV, respectively, which correspond to the conditions of our experiment. Good agreement with the experiment is obtained for the first four lines. For line 5, our calculations predict very small dichroism while the experiment shows dichroism similar to that for line 4. The reason for this discrepancy is unclear.

The energy dependence of the LMDAD is presented in Fig. 4. Here the experimental (symbols) and theoretical (curves) values of relative LMDAD [see Eq. (7)] are shown for the two first lines of the $4p$-photoionization spectrum. The calculation of the relative LMDAD is performed with the same orientation parameter ($\mathcal{A}_{10} = 0.25$) as before. The experimental points were normalized in such a way that the curve for the second line comes through the experimental point at the photon energy of 60 eV. Qualitatively, the theory agrees with the experiment. In the considered photon energy region, the relative dichroism changes its sign both in the calculations and in the experiment. However, in the calculations, the crossing point where the dichroism vanishes is shifted to higher energies by about 8 eV relative to the experiment. Presumably this shift is related to the shift of the calculated Cooper minimum. We note here that, at least in the nonrelativistic limit (pure LS-coupling), the LMDAD should vanish at the Cooper minimum. Indeed, as follows from the theory in Ref. [33], the LMDAD is a pure interference effect. It disappears when only one partial wave contributes. Thus it should be exactly zero at the energy where d-wave amplitude turns to zero. In the relativistic case, small contributions of relativistic components of the d-wave amplitude can slightly shift the position of LMDAD zero-crossing from the position of the Cooper minimum in the cross section. Nevertheless,

we think that the measurements of the zero-crossing in energy dependence of LMDAD is a very convenient and accurate method for determining the position of the Cooper minimum.

V. CONCLUSIONS

In summary, we report the first measurement of the angular distribution of photoelectrons from $4p$ photoionization of free Rb atoms and the linear magnetic dichroism in the angular distribution for the laser-oriented Rb ground state in the photon energy range of 50–100 eV. A high energy resolution of the experiment allows us to perform the measurements for all fine-structure components of the first ionic multiplets. The experimental results are compared with the MCDF calculations. In general, the calculations reproduce well the experimental values of the angular anisotropy parameters of $4p$ photoelectrons and the relative LMDAD as well as their energy dependence in the considered energy range. In the energy dependence of LMDAD, we observed the zero-crossing connected with the Cooper minimum of the cross section. The zero-crossing of LMDAD can be used as a convenient and accurate method for measuring the position of the Cooper minimum.

ACKNOWLEDGMENTS

The authors are grateful to the staff of MAX-laboratory for their assistance during the experiment. We are indebted to S. Svensson for his support in the laser experiment. We thank M. Vapa for his help in fitting the spectra. J. N. would like to thank Magnus Ehrnrooth's Foundation for the financial support during the work. N. M. K. gratefully acknowledges the hospitality of Oulu University and the financial support of the Research Council for Natural Sciences of the Academy of Finland. This work was financially supported by the European Community Research Infrastructure Action under the FP6 Structuring the European Research Area Program (through the Integrated Infrastructure Initiative Integrating Activity on Synchrotron and Free Electron Laser Sciences).

[1] F. J. Wuilleumier and M. Meyer, J. Phys. B **39**, R425 (2006).
[2] D. Cubaynes, M. Meyer, A. N. Grum-Grzhimailo, J.-M. Bizau, E. T. Kennedy, J. Bozek, M. Martins, S. Canton, B. Rude, N. Berrah, and F. J. Wuilleumier, Phys. Rev. Lett. **92**, 233002 (2004).
[3] J. Schulz, M. Tchaplyguine, T. Rander, O. Björneholm, S. Svensson, R. Sankari, S. Heinäsmäki, H. Aksela, S. Aksela, and E. Kukk, Phys. Rev. A **72**, 010702(R) (2005).
[4] D. Cubaynes, S. Guilbaud, F. J. Wuilleumier, M. Meyer, E. Heinecke, K. Riek, P. Zimmermann, M. Yalcinkaya, S. Fritzsche, S. I. Strakhova, and A. N. Grum-Grzhimailo, Phys. Rev. A **80**, 023410 (2009).
[5] A. N. Grum-Grzhimailo, E. V. Gryzlova, D. Cubaynes, E. Heinecke, M. Yalcinkaya, P. Zimmermann, and M. Meyer, J. Phys. B **42**, 171002 (2009).
[6] K. Jänkälä, R. Sankari, J. Schulz, M. Huttula, A. Caló, S. Heinäsmäki, S. Fritzsche, T. Rander, S. Svensson, S. Aksela, and H. Aksela, Phys. Rev. A **73**, 022720 (2006).
[7] M. Meyer, D. Cubaynes, F. J. Wuilleumier, E. Heinecke, T. Richter, P. Zimmermann, S. I. Strakhova, and A. N. Grum-Grzhimailo, J. Phys. B **39**, L153 (2006).
[8] J. Schulz, M. Tchaplyguine, T. Rander, H. Bergersen, A. Lindblad, G. Öhrwall, S. Svensson, S. Heinäsmäki, R. Sankari, S. Osmekhin, S. Aksela, and H. Aksela, Phys. Rev. A **72**, 032718 (2005).
[9] K. Jänkälä, J. Schulz, M. Huttula, A. Caló, S. Urpelainen, S. Heinäsmäki, S. Fritzsche, S. Svensson, S. Aksela, and H. Aksela, Phys. Rev. A **74**, 062704 (2006).
[10] J. Schulz, M. Määttä, S. Heinäsmäki, M. Huttula, R. Sankari, E. Kukk, T. Rander, S. Svensson, S. Aksela, and H. Aksela, Phys. Rev. A **73**, 062721 (2006).
[11] J. Schulz, E. Loos, M. Huttula, S. Heinäsmäki, S. Svensson, S. Aksela, and H. Aksela, Europhys. Lett. **83**, 53001 (2008).
[12] J. Niskanen, M. Huttula, S. Heinäsmäki, J. Schulz, S. Urpelainen, K. Jänkälä, A. Moise, M. Alagia, L. Avaldi, K. C. Prince, R. Richter, S. Aksela, and H. Aksela, J. Phys. B **42**, 175001 (2009).
[13] N. A. Cherepkov, V. V. Kuznetsov, and V. A. Verbitskii, J. Phys. B **28**, 1221 (1995).
[14] N. M. Kabachnik, J. Electron Spectrosc. Relat. Phenom. **79**, 269 (1996).
[15] M. Bässler, A. Ausmees, M. Jurvansuu, R. Feifel, J.-O. Forsell, P. de Tarso Fonseca, A. Kivimäki, S. Sundin, S. L. Sorensen, R. Nyholm, O. Björneholm, S. Aksela, and S. Svensson, Nucl. Instrum. Methods Phys. Res. A **469**, 382 (2001).
[16] M. Huttula, M. Harkoma, E. Nõmmiste, and S. Aksela, Nucl. Instrum. Methods Phys. Res. A **467**, 1514 (2001).
[17] M. Huttula, S. Heinäsmäki, H. Aksela, E. Kukk, and S. Aksela, J. Electron Spectrosc. Relat. Phenom. **156**, 270 (2007).
[18] R. E. Honig and D. A. Kramer, RCA Rev. **30**, 285 (1969).
[19] S. Baier, A. N. Grum-Grzhimailo, and N. M. Kabachnik, J. Phys. B **27**, 3363 (1994).
[20] V. V. Balashov, A. N. Grum–Grzhimailo, and N. M. Kabachnik, *Polarization and Correlation Phenomena in Atomic Collisions* (Kluwer Academic/Plenum Publishers, New York, 2000).
[21] I. P. Grant, in *Methods in Computational Chemistry*, edited by S. Wilson (Plenum Press, New York, 1988), Vol. 2, p. 1.
[22] F. A. Parpia, C. Froese Fischer, and I. P. Grant, Comput. Phys. Commun. **94**, 249 (1996).
[23] S. Fritzsche, C. Froese Fischer, and G. Gaigalas, Comput. Phys. Commun. **148**, 103 (2002).
[24] S. Fritzsche, H. Aksela, C. Z. Dong, S. Heinäsmäki, and J. E. Sienkiewicz, Nucl. Instrum. Methods Phys. Res. B **205**, 93 (2003).
[25] S. Fritzsche, Phys. Scr. T **100**, 37 (2002).
[26] S. Fritzsche, B. Fricke, and W.-D. Sepp, Phys. Rev. A **45**, 1465 (1992).

[27] S. Fritzsche, J. Electron Spectrosc. Relat. Phenom. **114**, 1155 (2001).
[28] S. Fritzsche, J. Nikkinen, S.-M. Huttula, H. Aksela, M. Huttula, and S. Aksela, Phys. Rev. A **75**, 012501 (2007).
[29] S. Heinäsmaki, K. Jänkälä, and J. Niskanen, J. Phys. B **42**, 085002 (2009).
[30] NIST Atomic Spectra Database http://physics.nist.gov/PhysRefData/ASD/.
[31] J. W. Cooper, Phys. Rev. **128**, 681 (1962).
[32] J. Tulkki, S. Aksela, H. Aksela, E. Shigemasa, A. Yagishita, and Y. Furusawa, Phys. Rev. A **45**, 4640 (1992).
[33] A. Verweyen, A. N. Grum-Grzhimailo, and N. M. Kabachnik, Phys. Rev. A **60**, 2076 (1999).
[34] Ph. Wernet, J. Schulz, B. Sonntag, K. Godehusen, P. Zimmermann, A. N. Grum-Grzhimailo, N. M. Kabachnik, and M. Martins, Phys. Rev. A **64**, 042707 (2001).